Environ Monit Assess (2018) 190: 594
https://doi.org/10.1007/s10661-018-6970-2

Real-time reservoir operation using data mining techniques

Omid Bozorg-Haddad · Mahyar Aboutalebi · Parisa-Sadat Ashofteh · Hugo A. Loáiciga

Received: 11 May 2018 / Accepted: 5 September 2018 / Published online: 19 September 2018

Abstract The optimal operation of hydropower reservoirs is essential for the planning and efficient management of water resources and the production of hydroelectric energy. Various techniques such as the genetic algorithm (GA), artificial neural networks (ANN), support vector machine (SVM), and dynamic programming (DP) have been employed to calculate reservoir operation rules. This paper implements the data mining techniques SVM and ANN to calculate the optimal release rule of hydropower reservoirs under "forecasting" and "non-forecasting" scenarios. The employment of data mining techniques accounting for data uncertainty to calculate optimal hydropower reservoir operation is novel in the field of water resource systems analysis. The optimal operation of the Karoon 3 reservoir, Iran, serves as a test of the proposed methodology. The upstream streamflow, storage records, and several lagged variables are model inputs. Data obtained from solving the reservoir optimization problem with nonlinear programming (NLP) are applied to train (calibrate) the SVM, and ANN, SVM, and ANN are executed in the "non-forecasting" scenario based on all inputs along with their time-lagged variables. In contrast, current parameters are removed from the set of inputs in the "forecasting" scenario. The results of the SVM model are compared with those of the ANN model with the correlation coefficient (*R*), the mean error (*ME*), and the root mean square error (*RMSE*). This paper's results indicate performance of the SVM is better than that of the ANN model by 1.5%, 400%, and 10% with respect to the *R*, *ME*, and *RMSE* diagnostic statistics, respectively. In addition, SVM and ANN overcome data uncertainty ("forecasting" scenario) to produce optimal reservoir operation.

Keywords Real-time reservoir operation · Hydropower · Rule curve · Support vector machine · Artificial neural network

O. Bozorg-Haddad (✉) · M. Aboutalebi
Department of Irrigation & Reclamation Engineering, Faculty of Agricultural Engineering & Technology, College of Agriculture & Natural Resources, University of Tehran, Karaj, Tehran, Iran
e-mail: OBHaddad@ut.ac.ir

M. Aboutalebi
e-mail: Aboutalebi@ut.ac.ir

P.-S. Ashofteh
Department of Civil Engineering, University of Qom, Qom, Iran
e-mail: PAshofteh@ut.ac.ir

H. A. Loáiciga
Department of Geography, University of California, Santa Barbara, CA 93106, USA
e-mail: Hugo.Loaiciga@ucsb.edu

Introduction

Planning and optimal operation of water resource systems plays a crucial role in today's world (Ahmadi et al. 2015a, b; Akbari-Alashti et al. 2014; Beygi et al. 2014; Bozorg-Haddad et al. 2013, 2015a, b; Farhangi et al. 2012;

Fallah-Mehdipour et al. 2013a, b, 2014; Jahandideh-Tehrani et al. 2015; Orouji et al. 2013, 2014a, b). This role is accentuated by the widespread scarcity of groundwater, surface water, and other water resources (Loáiciga 2015). Reservoir operation rules dictate the amount of water that must be stored or released according to variable operating conditions. Reservoir operators specify the rate of water release based on the reservoir storage, inflow to the reservoir, and downstream water requirement using rule curves. The rule curve is a function between a reservoir's state and the decision (operational) variables. The state variables are reservoir storage and inflow to the reservoir, and the decision variable is the rate of reservoir release.

Many optimized reservoir operation rules can be found in studies by Bower et al. (1962), Loucks et al. (1981), Yeh (1985), Oliveria and Loucks (Oliveira and Loucks 1997), and Bolouri-Yazdeli et al. (2014), to cite a few examples. Cai et al. (2001) described strategies for solving large nonlinear water resource model management, which combined genetic algorithms (GAs) with linear programming (LP). Tung et al. (2003) proposed a procedure to use genetic algorithm to optimize operation rules for the Liyutan Reservoir in Taiwan. Chen (2003) applied a real coded genetic algorithm (RGA) to obtain the 10-day operating rule curves for a reservoir system in Taiwan. Mousavi et al. (2007) compared the methods of ordinary least-squares regression (OLSR), fuzzy regression (FR), and adaptive network-based fuzzy inference system (ANFIS) in inferring operating rules for a reservoir operation optimization problem. Bozorg-Haddad et al. (2008a) evaluated the performance of the honey-bee mating optimization (HBMO) algorithm in highly non-convex hydropower system design and operation.

Bozorg-Haddad et al. (2008b) applied the HBMO algorithm to extract the linear monthly operation rules of reservoirs for irrigation and hydropower purposes. The release rules for each month were considered as a linear function of the reservoir storage as well as the current monthly inflow to the reservoir. Pinthong et al. (2009) developed a hybrid genetic and neuro-fuzzy computing algorithm to enhance efficiency of water management for a multi-purpose reservoir system. The genetic algorithm was applied to search for the optimal input combination of a neuro-fuzzy system. Garousi-Nejad and Bozorg-Haddad (2015) and Garousi-Nejad et al. (2016a, 2016b) reported the application of a modified firefly algorithm to the operational reservoir problem.

Data mining is the application of automated search knowledge to find new and valuable information in large data sets. In other words, data mining is the interaction between humans and computers in the quest to discover information hidden within large data volumes. The primary goals of data mining are discovery, classification, and prediction. ANN and SVM are the most important tools in data mining (Babovic 2004).

Yu et al. (2004) presented a new tool combining chaos theory and SVM and applied it to the analysis of time series in a large database. Asefa et al. (2006) employed SVM to forecast hourly and seasonal flow. Behzad et al. (2009) evaluated the performance of SVM and ANN in forecasting streamflow of the Bakhtiyari River (in Iran). The results were compared with those of ANN and of ANN integrated with genetic algorithm (ANN-GA) models. Yoon et al. (2011) predicted groundwater level (GWL) fluctuations in a coastal aquifer in Korea with ANN and SVM. Singh et al. (2011) applied support vector classification (SVC) and regression (SVR) models to optimize a water-quality monitoring program. Wei (2012) presented wavelet SVMs for forecasting the hourly water levels at gauging stations using classical Gaussian and wavelet SVMs. Wang et al. (2013) linked the PSO algorithm to SVM to improve rainfall-runoff prediction. Li et al. (2014) predicted real-time floods in real time combining SVM and a data-assimilation method. Ahmadi et al. (2015a, b) implemented an input selection technique for forecasting long-lead precipitation. Yang et al. (2016) presented a robust method incorporating the Classification and Regression Tree (CART) to simulate the outflow of nine major reservoirs in California. Their results revealed the enhanced CART could provide a better performance over random forest for peak flow simulation. Yang et al. (2017) compared the performance of SVM, ANN, and random forest (RF) techniques to predict 1 month-ahead reservoir inflow. They found RF performed better than SVM and ANN, with climatic indices improving the forecasting of monthly and seasonal reservoir inflows. Other applications of SVM to water resources management are found in reviews by Aboutalebi and Bozorg-Haddad (2015) and Aboutalebi et al. (2015, 2016a, b, c).

Observational data are required for model calibration when applying data mining tools such as SVM and ANN. The NLP technique is applied in this study to generate observed data for calibration purposes. In other words, an optimization model of hydropower reservoir operation is solved with NLP. The optimized solution set obtained with NLP is applied as the target data to calibrate the SVM and ANN model. Subsequently, an optimized reservoir-operation rule is calculated for each operating period with the calibrated SVM based on the dependency between variables, such as that between reservoir storage and reservoir inflow (these are the input data), and then applying the rate of release obtained with NLP (these are the target data). This paper evaluates the sensitivity of SVM and ANN to the lack of information for simulating optimized reservoir operation. The sensitivity evaluation relies on two approaches to cope with reservoir inflow uncertainty. The first approach (the forecasting approach) is dependent on inflow forecasting, and the second approach (non-forecasting approach) is independent of inflow forecasting. Input variables in the forecasting approach include inflow forecasts made in the current period. The non-forecasting approach does not include inflow forecasts. The reason for considering forecasting and non-forecasting approaches is to compare the effect that inflow forecasting has on the computation of optimal rules for reservoir operation. NLP cannot be executed without the knowledge of current storage and inflow. Therefore, if SVM and ANN can achieve a reservoir operation rule similar to that from NLP optimization, this constitutes a significant advantage of data mining techniques versus the gradient-based NLP. Moreover, The SVM and ANN models are assessed at monthly and annual time scales. To accomplish these goals, the observed data were classified as types 1 and 2 in the application of SVM and ANN. Type 1 data are long-term monthly time series. Type 2 data are average monthly values. Therefore, for each approach, there is one time series of type 1 and there are 12 time series of type 2. The reservoir-operation rule results of the SVM model are compared those calculated with the ANN model.

Methodology

This paper's methodology consists of three steps. The first is modeling a hydropower system and calculating a reservoir operation rule with the NLP method. The second involves SVM and ANN models' calibrations, testing, and specification of model parameters. The last is implementing and comparing the SVM and ANN models and their results.

Optimal reservoir operation

A reservoir operation rule curve for hydropower production is calculated using NLP. The objective function of the reservoir operation model minimizes the normalized power production deficit:

$$\text{MinimizeDef} = \sum_{t=1}^{T}\left(1 - \frac{P_t}{PPC}\right)^2 \quad (1)$$

in which Def = objective function, P_t = power generated in period t, PPC = power plant capacity (10^6 watt), and T = number of operation periods.

The generated power in each month (period t) is calculated with Eq. (2):

$$P_t = g \times E \times \frac{Rp_t}{PF \cdot M_t} \times \frac{\left(\overline{H}_t - TW\right)}{1,000} \quad (2)$$

in which g = acceleration of gravity (9.81 m/s^2), E = efficiency of the power plant, Rp_t = inflow to power plant in period t (10^6 m^3), PF = power plant factor, M_t = conversion coefficient from 10^6 m^3 to cubic meter per second in period t, $\overline{H}_t$ = average water level (m) in reservoir at the beginning of period t (meters above mean sea level), and TW = average elevation of the tailwater (m) in period t (meters above mean sea level).

The constraints of the model are:

Conservation of volume (continuity equation):

$$S_{t+1} = S_t + Q_t - Sp_t - R_t - L_t\left(\overline{S}_t\right) \quad (3)$$

Constraints on reservoir storage:

$$S_{\min} \le S_t \le S_{\max} \quad (4)$$

Constraints on reservoir releases:

$$R_{\min} \le R_t \le R_{\max} \quad (5)$$

Constraints on hydropower production:

$$0 \le P_t \le PPC \quad (6)$$

Specification of reservoir releases:

$$Sp_t = \begin{cases} S_{\max} - S_{t+1} & \text{if} \quad S_{t+1} \ge S_{\max} \\ 0 & \text{if} \quad S_{t+1} < S_{\max} \end{cases} \quad (7)$$

in which S_t and S_{t+1} = reservoir storage volume at the beginning of period t and $t + 1$, respectively (10^6 m^3), Q_t = inflow to reservoir during period t (10^6 m^3), Sp_t = spillage from reservoir in period t (10^6 m^3), R_t =

reservoir release in period t (10^6 m^3), $L_t(\overline{S}_t)$ = evaporation in period t that it calculated with a set of implicit nonlinear equations (10^6 m^3), S_{max} = maximum volume of the reservoir storage (10^6 m^3), S_{min} = dead volume of reservoir storage (10^6 m^3), and R_{max} and R_{min} = maximum and minimum release from the power plant (10^6 m^3), respectively.

The reservoir's water surface in each time periods is a third-degree power function of the storage volume at the beginning of each time period according to Eq. (8). The amount of evaporation losses is calculated as the product of the evaporation depth and average water surface as written in Eqs. (9) and (10):

$$A_t = a_0 \times S_t^3 + a_1 \times S_t^2 + a_2 \times S_t + a_3 \quad (8)$$

$$L_t(S_t, S_{t+1}) = Ev_t \times \overline{A}_t \quad (9)$$

$$\overline{A}_t = \frac{A_t + A_{t+1}}{2} \quad (10)$$

in which A_t, A_{t+1} = water surface area of reservoir at the beginning of periods t and $t+1$, respectively (10^6 m^2); $\overline{A}_t$ = average of water surface area (10^6 m^2); Ev_t = evaporation depth in period t (m); and a_0, a_1, a_2, and a_3 = coefficients of the surface-storage Eq. (8).

The reservoir water level is calculated as a third-degree polynomial of the of reservoir storage:

$$H_t = b_0 \times S_t^3 + b_1 \times S_t^2 + b_2 \times S_t + b_3 \quad (11)$$

in which H_t = water level of reservoir in period t (m); and b_0, b_1, b_2, and b_3 = coefficients of the water level-storage.

The reservoir model embodied by Eqs. (1)–(11) is nonlinear. It was solved with the LINGO 11.0 NLP software.

ANN

An ANN is an information processing system that attempts to replicate the activity of the human brain employing interconnected data structures that emulate the function of the neurons. Data structures are called nodes. Nodes in a neural network can be active (ON or 1) or disabled (Off or 0). Each edge (synapses or connections between nodes) has a specified weight. Edges with positive weight stimulate or activate the next active node, while edges with negative weight idle or block (if it is active) the next connected node.

The multi-layer perceptron (MLP) network is one of the most common arrangements of a neural network. In this network, each neuron in each layer is connected to all neurons of the previous layer and the output of each layer constitutes input vectors of the next layer. Sigmoid functions or hyperbolic tangents are common in MLP and the law of error backpropagation (BP) is employed to train (that is, calibrate) them. Neural network training is a process whereby the weights of connections are optimized in a continuous process to consolidate the network. Assessments of the learning and network performance with trained and untrained inputs are carried out for validation purposes. The standard assessment procedure is to use part of the existing data for training (calibration) and the remainder of the data for testing of the network.

Support vector machine

Support vector machine (SVM) is a learning process that employs a hypothesis space called the feature space that features multi-dimensional linear functions. The SVM theory was introduced by Vapnik (1995) as a method for data classification and regression.

The linear SVM

This section introduces SVM theory and its use for regression and forecasting in the linear form introduced by Vapnik (1995) relying on the ε-insensitive error function to create the sparseness property of support vector regression (SVR), as follows:

$$|y - f(x)| = \begin{cases} 0 & if \ \ |y - f(x)| \le \varepsilon \\ |y - f(x)| - \varepsilon = \xi & \text{otherwise} \end{cases} \quad (12)$$

in which y = observed data, $f(x)$ = data estimated with SVR, x = input data, ε = sensitivity function, and ξ = error value considered for estimates outside the range ($-\varepsilon$ to $+\varepsilon$).

The function $f(x)$ in Eq. (12) is defined by Eq. (13):

$$f(x) = w^T.x + b \quad (13)$$

in which w = weighting vector applied to vector of variables x, b = deviation, and T = the transpose symbol applied to vectors or matrices.

SVR minimizes the ε-insensitive error function and weight vector w. Therefore, the objective function and constraints of SVR are defined as follows:

$$\text{Min}: \quad \frac{1}{2}\cdot\|w\|^2 + C\cdot\sum_{i=1}^{m}\left(\xi_i+\xi_i^*\right) \tag{14}$$

$$\text{Subjectto}: \quad \begin{array}{l}\left(w^T\cdot x+b\right)-y_i\leq\varepsilon+\xi_i \\ y_i-\left(w^T\cdot x+b\right)\leq\varepsilon+\xi_i^* \\ \xi_i,\xi_i^*\geq 0\end{array} \tag{15}$$

in which $\|\|$ = symbol for vector length, C = penalty factor, m = number of training data, and ξ and ξ^* = penalties considered for estimated outside the range ($-\varepsilon$ to $+\varepsilon$), respectively.

The penalties applied to estimates are shown in Fig. 1, where it is seen that the estimates in the range ($-\varepsilon$ to $+\varepsilon$) are not penalized, and estimates outside that range are penalized. The input variables to SVR are x ($x\in R^n$), and its output variables are y ($y\in R$).

A Lagrangian objective function (L) is implemented to solve the optimization problem expressed by Eqs. (14)–(15):

$$L\equiv\frac{1}{2}\|w\|^2 + C\cdot\sum_{i=1}^{m}\left(\xi_i+\xi_i^*\right)-\sum_{i=1}^{m}\left(\eta_i\xi_i+\eta_i^*\xi_i^*\right)-\sum_{i=1}^{m}\alpha_i\cdot\left[\varepsilon+\xi_i+y_i-\left(w^T\cdot x+b\right)\right]-\sum_{i=1}^{m}\alpha_i^*\cdot\left[\varepsilon+\xi_i^*-y_i+\left(w^T\cdot x+b\right)\right] \tag{16}$$

Subject to

$$\alpha_i^*,\eta_i^*\geq 0 \tag{17}$$

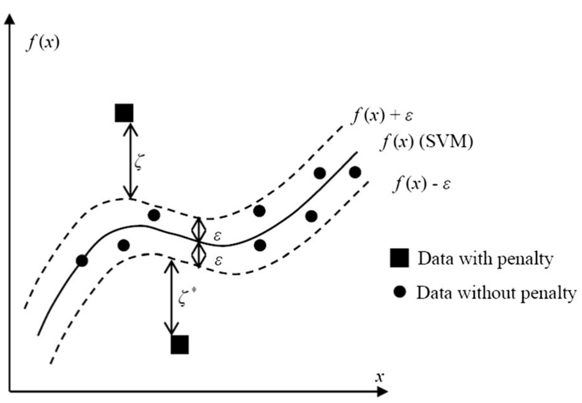

Fig. 1 Penalized and non-penalized data

in which α_i^* ($\alpha^*\in R^n$), α_i, η_i^*, and η_i = Lagrange multipliers.

The partial derivatives of the Lagrangian function with respect to ξ_i^*, ξ_i, b, and w must be zero:

$$\partial L/\partial b=\sum_{i=1}^{m}\left(\alpha_i-\alpha_i^*\right)=0 \tag{18}$$

$$\partial L/\partial w=w-\sum_{i=1}^{m}\left(\alpha_i-\alpha_i^*\right)\cdot x_i=0 \tag{19}$$

$$\partial L/\left(\partial\xi_i,\partial\xi_i^*\right)=C-\alpha_i^*-\eta_i^*=0 \tag{20}$$

in which $\partial L/\partial b$ = partial derivative of function L with respect to variable b, $\partial L/\partial w$ = partial derivative of function L with respect to variable w, and $\partial L/\left(\partial\xi_i,\partial\xi_i^*\right)$ = partial derivative of function L with respect to variables of ξ_i^* and ξ_i.

The value of w is calculated with Eq. (21):

$$w=\sum_{i=1}^{m}\left(\alpha_i^*-\alpha_i\right)\cdot x_i \tag{21}$$

Substituting Eqs. (18)–(20) into Eq. (16) produces the following optimization problem in terms of the coefficients α_i and α_i^*:

$$\text{Max}: \quad -\frac{1}{2}\cdot\sum_{i,j=1}^{m}\left(\alpha_i^*-\alpha_i\right)\cdot\left(\alpha_j^*-\alpha_j\right)\cdot\left(x_i^T-x_j\right)-\varepsilon\cdot\sum_{i=1}^{m}\left(\alpha_i^*-\alpha_i\right)+\sum_{i=1}^{m}y_i\cdot\left(\alpha_i^*-\alpha_i\right) \tag{22}$$

$$\text{Subjectto}: \quad \sum_{i=1}^{m}\left(\alpha_i-\alpha_i^*\right)=0 \quad \text{and} \quad \alpha_i,\alpha_i^*\in[0,C] \tag{23}$$

The estimation function of the observed variable of y is given by Eq. (24) once the coefficients α_i and α_i^* are solved for:

$$f(x)=\sum_{i=1}^{m}\left(\alpha_i^*-\alpha_i\right)\cdot\left(x_i^T\cdot x\right)+b \tag{24}$$

Cristianini and Shawe-Taylor (2000) demonstrated that Eq. (24) is a convex constrained quadratic programming problem, and thus it guarantees a unique solution.

The Kuhn-Tucker (KT) conditions are used to calculate b in Eq. (24). These conditions state that the product of Lagrange multipliers and constraints must equal zero at the solution point:

$$\alpha_i \cdot \left[\varepsilon + \xi_i + y_i - \left(w^T \cdot x_i + b\right)\right] = 0 \tag{25}$$

$$\alpha_i^* \cdot \left[\varepsilon + \xi_i^* + y_i - \left(w^T \cdot x_i + b\right)\right] = 0 \tag{26}$$

$$(C - \alpha_i) \cdot \xi_i = 0 \tag{27}$$

$$\left(C - \alpha_i^*\right) \cdot \xi_i^* = 0 \tag{28}$$

The following results follow from the KT conditions:

(1) The coefficient $\alpha_i^*$is equal to C when differences between the variables (x_i, y_i) are outside the range ($-\varepsilon$ to $+\varepsilon$), so that $\left(\xi_i, \xi_i^* > 0\right)$,
(2) Lagrange multipliers are never simultaneously nonzero, α_i, $\alpha_i^* \neq 0$
(3) The coefficients α_i and α_i^* equal zero for estimates within the range ($-\varepsilon$ to $+\varepsilon$).
(4) The penalties ξ_i and ξ_i^* are equal to zero when $\alpha_i, \alpha_i^* \in (0, C)$, and thus the factors within brackets in Eqs. (25) and (26) must equal to zero. Therefore, the value of b is calculated with Eqs. (29) and (30):

$$b = y_i - \left(w^T \cdot x_i + b\right) + \varepsilon \quad , \quad \alpha_i \in (0, C) \tag{29}$$

$$b = y_i - \left(w^T \cdot x_i + b\right) + \varepsilon \quad , \quad \alpha_i^* \in (0, C) \tag{30}$$

Only one of the Lagrange multipliers within (0, C) is selected and inserted in either of Eq. (29) or (30) to calculate the value of b.

With regard to result (2) of the KT conditions written above, all samples located within the range of ($-\varepsilon$ to $+\varepsilon$) have Lagrange multipliers $\left(\alpha_i, \alpha_i^*\right)$ equal to zero. Thus, it is not necessary to calculate all the values of w in SVR. The estimates that have nonzero Lagrange multipliers are called support vectors (SVs). Estimates in the range ($-\varepsilon$ to $+\varepsilon$) do not contribute to the solution of an optimization problem. Thus, they are removed from further analysis.

Nonlinear SVM

Transfer functions are employed to fit linear functions to data when it is not possible to fit linear functions to training data. Transfer functions in SVM are called Kernel functions. Thus, the estimation function in SVM replaces Eq. (24) with Eq. (31):

$$f(x) = \sum_{i=1}^{m} \left(\alpha_i^* - \alpha_i\right) \cdot K(x_i, x) + b \tag{31}$$

in which K = Kernel function.

Dibike et al. (2001) applied Kernel functions in the SVR model for modeling of rainfall-runoff process. They concluded that radial basis functions (RBF) have better performance than other Kernel functions. Han and Cluckie (2004) deduced that the RBF's centralized property enables it to perform regressions effectively. Other studies, such as those of Asefa et al. (2005), Lin et al. (2006), Yu et al. (2006), and Khalil et al. (2005) relevant to hydrologic modeling and forecasting with SVR established the good performance of the RBFs. Equation (32) is exemplary of an RBF:

$$K(x, x_i) = \exp\left(-\frac{|x - x_i|^2}{2\gamma^2}\right) \tag{32}$$

in which γ = RBF parameter.

A flow diagram of SVR is shown in Fig. 2. The figure depicts the various stages of regression performed by SVR. Input vectors are input to the Kernel functions. Next, the inner product of the support vectors is performed by the Kernel function. Lastly, the total inner products are calculated with weighting values (Lagrange multipliers) and the estimated output is calculated by adding b to those values. This process is very similar to that of a neural network with the difference that there is only one hidden layer in SVR.

Determination of the SVM parameters

The SVM parameters include C, ε (SVM model parameters), and parameters related to the Kernel function used (such as the parameter γ of the RBF Kernel function). The optimal choice of the SVM parameters is essential for its adequate performance. The choice of C and ε usually is left to the user and it is based on prior information or experience with the workings of evolutionary algorithms. However,

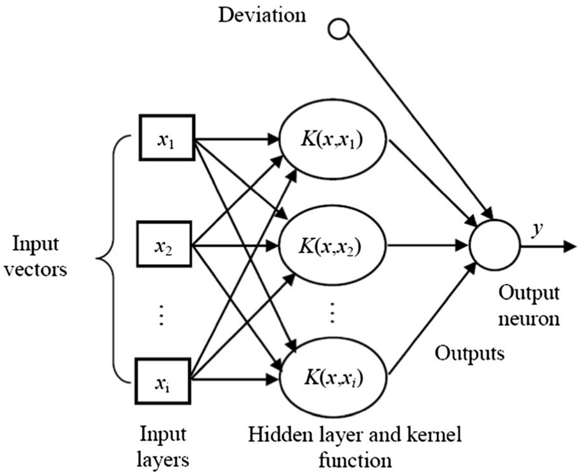

Fig. 2 Schematic structure of SVR

in this paper, we implemented a trial and error method to find the best values of SVM and ANN parameters. Moreover, the kernel functions are chosen based on prior experience document in the specialized SVM and ANN literature.

The study area

The Karoon 3 dam is Iran's largest dam, located on the Karoon River in southwestern Iran. The Karoon 3 dam meets hydropower production and flood control functions. The Karoon 3's power plant has an installed capacity equal to 2000 MW and generates an average annual energy equal to 4137 gigawatt hour for peak-time electricity supply. Energy shortages, particularly during peak-use times, have been mostly resolved since the dam's construction in 2005. Reservoir inflow data for 44 years (1957–2000) were used to calculate an optimal reservoir operation rule. The 40-year average monthly inflow and evaporation in to the Karoon 3 dam are listed in Table 1. It is seen in Table 1 that April and October have the largest and smallest inflows, respectively. Also, the largest and smallest evaporation in the reservoir occur in July and January, respectively. The Karoon 3's power plant has an efficiency equal to 92%, a plant factor equal to 0.25, and a downstream water level (tailwater elevation) equal to 665 m above mean sea level.

Methodology

The optimization model is first solved with the Lingo software. Subsequently, the data or output obtained from the software is normalized in the range − 1 to + 1. The Box-Cox transformation function written in Eq. (33) is applied in this study for data normalization (Box and Cox 1964):

$$x^{'} = f(x,\lambda) = \frac{x^{\lambda}-1}{x} \tag{33}$$

in which $x^{'}$ = normalized data, x = output variables of the optimization model, and λ = transformation function parameter.

The MATLAB software 2012b was implemented in this work for data normalization. This software estimates the optimal value of the transformation function parameter.

After normalizing the data, they must be standardized. For this purpose, Eq. (34) is used:

$$x^{''} = \frac{x^{'}-\mu}{\sigma} \tag{34}$$

in which μ = average value of the data being standardized, σ = standard deviation of the data, and $x^{''}$ = standardized data.

Percentages equal to 70% and 30% of the total data values were chosen for data training and testing, respectively. The data for training and testing are chosen

Table 1 40-year average monthly reservoir inflow and reservoir evaporation data

Month	Oct	Nov	Dec	Jan	Feb	Mar	Apr	May	Jun	Jul	Aug	Sep
Average inflow (10^6 m^3)	333.2	407.2	577.8	589.9	805.7	1225.3	1795.0	1550.8	1022.6	674.9	481.6	367.3
Average evaporation (mm)	204.6	99.5	68.3	56.2	59.2	76.6	111	169.9	251	311.6	293.9	277

randomly. The type 1 forecasting approach predicts reservoir release based on values of storage and reservoir inflow in periods t, t-1, t-2, and t-3:

$$R_t = f(S_t, S_{t-1}, S_{t-2}, S_{t-3}, Q_t, Q_{t-1}, Q_{t-2}, Q_{t-3}) \quad t = 1, 2, 3, \ldots, 524 \tag{35}$$

The type 1 non-forecasting approach predicts release based on values of storage in periods t, t-1, t-2, and t-3, and values of reservoir inflow in periods t-1, t-2, and t-3 (notice the current-period inflow Q_t does not enter in this approach):

$$R_t = f(S_t, S_{t-1}, S_{t-2}, S_{t-3}, Q_{t-1}, Q_{t-2}, Q_{t-3}) \quad t = 1, 2, 3, \ldots, 524 \tag{36}$$

The type 2 forecasting approach calculates the release based on average monthly reservoir storage and average monthly reservoir inflow in intervals m, m-1, m-2, and m-3:

$$R_m = f(S_m, S_{m-1}, S_{m-2}, S_{m-3}, Q_m, Q_{m-1}, Q_{m-2}, Q_{m-3}) \quad m = 1, 2, 3, \ldots, 44 \tag{37}$$

The type 2 non-forecasting approach calculates the reservoir release based on average monthly storage in intervals m, m-1, m-2, and m-3 and on average monthly reservoir inflow in intervals m-1, m-2, and m-3 (notice the current-period average inflow Q_m does not enter in this approach):

$$R_m = f(S_m, S_{m-1}, S_{m-2}, S_{m-3}, Q_{m-1}, Q_{m-2}, Q_{m-3}) \quad m = 1, 2, 3, \ldots, 44 \tag{38}$$

in which t and m = indices of the long-term time series (type 1 data) and of the average monthly time series (type 2 data), respectively.

The SVM and ANN were implemented in Tanagra 1.4.2 (Rakotomalala 2005) and MATLAB, respectively. The sigmoid function was chosen as the ANN transfer function. The RBF was applied as the Kernel function of the SVM. The number of hidden nodes and layers, and other parameters related to the transfer and Kernel functions were determined by trial and error leading to the parameters listed in Tables 2 and 3.

The forecasting and non-forecasting approaches were implemented with the SVM model and ANN. The SVM model was run with the forecasting and non-forecasting approaches [Eqs. (35) and (36)] based on type 1 data, and with Eqs. (37) and (38) based on type 2 data. The same procedure was employed to run the forecasting and non-forecasting approaches with ANN. The performance of the ANN and SVM models was evaluated with the R, ME, and $RMSE$ diagnostic statistics defined by Eqs. (39)–(41):

$$R = \frac{\sum_{t=1}^{n} \left(R_{0(t)} - \overline{R}_0\right) \cdot \left(R_{m(t)} - \overline{R}_m\right)}{\left[\sum_{t=1}^{n} \left(R_{0(t)} - \overline{R}_0\right)^2 \cdot \sum_{t=1}^{n} \left(R_{m(t)} - \overline{R}_m\right)^2\right]^{0.5}} \tag{39}$$

$$ME = \sum_{t=1}^{n} \frac{\left(R_{0(t)} - R_{m(t)}\right)^2}{R_{0(t)}} \tag{40}$$

$$RMSE = \sqrt{\frac{\sum_{t=1}^{n} \left(R_{0(t)} - R_{m(t)}\right)^2}{n}} \tag{41}$$

in which n = number of data values, $R_{0(t)}$ and $\overline{R}_0$ = release in period t and average release during operational period obtained with the NLP method, respectively, and $R_{m(t)}$ and $\overline{R}_m$ = release in period t and average release during operational period obtained from the SVM model, respectively.

Results

The objective function calculated with NLP equaled 44.8. Three diagnostic statistics R, ME, and $RMSE$ defined in Eqs. (39)–(41) for the non-forecasting and forecasting approaches are listed in Tables 4 and 5, respectively. It is seen in Table 4 the ANN and SVM non-forecasting models exhibited optimal performance in the training phase as measured by the three diagnostic statistics. In the training phase, the SVM model had R equal to 1 in October, February, June, August, and September, whereas the ANN model had R equal to 1 in January, February, July, and September. The ANN model had R larger than 0.9, except in February, March, May, and July. The SVM model had R larger than 0.9 except in March. The SVM model exhibited better performance than the ANN model in March.

Table 2 Model parameters of the non-forecasting approach

Model type	SVM				ANN
Non-forecasting	Number of support vectors	ε	γ	C	Number of neurons
Oct	30	0.0010	0.03	7	10
Nov	30	0.0010	0.10	4	15
Dec	30	0.0010	0.04	20	14
Jan	31	0.0010	0.60	10	17
Feb	31	0.0010	0.06	7	12
Mar	32	0.0100	0.29	8	17
Apr	15	0.0001	0.05	6	15
May	32	0.0010	0.11	8	19
Jun	32	0.0100	0.04	10	11
Jul	32	0.1500	0.30	9	16
Aug	26	0.0100	0.06	1	17
Sep	29	0.0100	0.10	8	14
Long-term time series	338	0.0100	0.16	7	19

Concerning the testing phase, it is seen in Table 4 that the difference between the values of the diagnostic statistics obtained with SVM and with the ANN non-forecasting models is considerable in July, December, February, October, January, and March. Specifically, the July R, ME, and RMSE values for the SVM model differed by 10, 170, and 60% from those obtained with the ANN model. The overall performance of the ANN and SVM models in the training and testing phases with the non-forecasting approaches is acceptable. Also, with regard to the type 1 data (long-term series) and type 2 data (monthly time series), it is seen in Table 4 that use of the monthly data produced an improved performance in the training and total (total = training and testing) phases, whereas there was no perceived improvement in the testing phase.

Table 3 Model parameters of the forecasting approach

Model type	SVM				ANN
Forecasting	Number of support vectors	ε	γ	C	Number of neurons
Oct	30	0.0010	0.028	9	11
Nov	30	0.0010	0.120	6	13
Dec	30	0.0010	0.100	15	15
Jan	31	0.0010	0.650	10	14
Feb	31	0.0010	0.100	9	18
Mar	32	0.0020	0.200	8	15
Apr	20	0.2000	0.070	7	16
May	32	0.0010	0.130	6	14
Jun	32	0.0010	0.070	10	15
Jul	32	0.0100	0.250	8	12
Aug	26	0.1500	0.090	2	16
Sep	29	0.0100	0.120	8	14
Long-term time series	338	0.0100	0.200	11	18

The results in Table 5 show the forecasting SVM model had R equal to 1 in December, January, February, June, and September, and the forecasting ANN model had R equal to 1 in October, November, January, March, April, May, August, and September in the training phase. This good performance is attributed to the use of the inflow variable in the current period as input variable in the forecasting approach [see Eq. (35)]. Concerning the testing phase, the ANN and SVM models had R larger than 0.9 in all months but May. In this same phase, there was a significant difference between the values of the diagnostic statistics of the SVM and ANN models in May, April, June, and January. Specifically, the *R*, *ME*, and *RMSE* of the SVM model differed by 8.5, 13, and 13% from those of the ANN model. It was determined that implementing monthly data improves performance. It is noted that this improvement is more pronounced with the ANN model,

Table 4 Values of *R*, *ME*, and *RMSE* for implementation of the non-forecasting approach

Time series	Model	Train			Test			Total		
		R (%)	*ME* (10^6 m^3)	*RMSE* (10^6 m^3)	*R* (%)	*ME* (10^6 m^3)	*RMSE* (10^6 m^3)	*R* (%)	*ME* (10^6 m^3)	*RMSE* (10^6 m^3)
Oct	ANN	0.988	37.720	25.848	0.927	84.524	57.339	0.973	122.243	38.211
	SVM	1.000	0.584	3.450	0.994	4.671	15.179	0.999	5.256	8.829
Nov	ANN	0.999	5.570	9.294	0.998	14.850	31.922	0.997	20.421	19.192
	SVM	0.991	37.885	23.984	0.996	14.595	30.275	0.991	52.480	26.047
Dec	ANN	0.994	32.743	26.021	0.907	91.283	81.836	0.971	124.026	49.971
	SVM	0.997	13.483	16.462	0.994	16.637	24.680	0.996	30.120	19.319
Jan	ANN	1.000	0.052	1.050	0.934	47.896	56.968	0.985	47.947	31.336
	SVM	0.997	11.106	16.380	0.990	7.767	23.360	0.995	18.873	18.766
Feb	ANN	1.000	4.031	8.549	0.858	134.785	93.892	0.959	138.536	51.538
	SVM	1.000	0.140	1.781	0.927	67.825	60.977	0.982	67.956	33.178
Mar	ANN	0.989	54.724	38.715	0.827	111.400	88.063	0.940	165.001	57.856
	SVM	0.992	10.281	17.329	0.869	69.790	70.544	0.954	80.067	41.011
Apr	ANN	0.999	1.375	6.166	0.951	45.207	53.625	0.973	46.536	29.604
	SVM	0.961	25.493	25.231	0.956	43.929	46.586	0.965	69.419	33.011
May	ANN	0.944	38.595	31.635	0.891	36.794	48.460	0.926	75.369	37.402
	SVM	0.998	1.089	5.191	0.908	13.713	29.463	0.979	14.801	16.597
Jun	ANN	0.995	3.189	9.174	0.946	101.732	68.489	0.975	104.786	38.016
	SVM	1.000	6.309	9.828	0.950	24.407	33.415	0.982	24.457	19.949
Jul	ANN	1.000	0.000	0.002	0.872	208.798	105.470	0.940	208.798	57.329
	SVM	0.989	27.397	22.766	0.973	39.848	46.085	0.982	67.240	31.506
Aug	ANN	1.000	0.000	0.000	0.924	92.790	63.480	0.978	92.790	34.505
	SVM	1.000	0.151	1.550	0.946	54.034	51.141	0.986	54.181	27.828
Sep	ANN	1.000	0.046	0.819	0.959	41.692	48.526	0.982	41.736	26.385
	SVM	1.000	0.775	4.109	0.993	10.301	23.538	0.997	11.075	13.251
Type 1	ANN	0.974	1100.717	45.315	0.950	600.882	53.936	0.968	1701.599	48.043
	SVM	0.994	232.734	20.938	0.979	249.524	35.184	0.990	482.258	26.008
Type 2	ANN	0.996	176.001	18.562	0.943	706.018	57.226	0.983	882.019	34.884
	SVM	0.997	124.876	13.891	0.974	313.941	38.652	0.992	438.817	24.089

which had a reduction in *R* of about 2% and other statistics were reduced by about one half.

The forecasting and non-forecasting approaches exhibited the minimal and maximal values of the *RMSE* for both the SVM and ANN models, respectively. The non-forecasting approach applied with the SVM model performed better than the forecasting approach applied with the ANN model, in most cases. The results obtained with monthly data (type 2 data) exhibited smaller RMSEs in the training and testing phases, in general, than those obtained with the long-term time series (type 1 data). The largest values of the *RMSE* were obtained with the non-forecasting ANN model in the testing phase in July and February. The training and testing phases exhibited minimal and maximal of *RMSEs*, respectively.

Average values of the diagnostic statistics *R*, *ME*, and *RMSE* calculated with the forecasting and non-forecasting approaches are listed in Table 6. According to Table 6, the non-forecasting approach estimates optimal release with acceptable precision compared to the forecasting approach, despite the lack of use of inflow variable in the current period as input variable [see Eq. (38)]. The use or lack of use of the inflow variable in the

Table 5 Values of *R*, *ME*, and *RMSE* for implementing the forecasting approach

Time series	Model	Train			Test			Total		
		R (%)	*ME* (10^6 m^3)	*RMSE* (10^6 m^3)	*R* (%)	*ME* (10^6 m^3)	*RMSE* (10^6 m^3)	*R* (%)	*ME* (10^6 m^3)	*RMSE* (10^6 m^3)
Oct	ANN	1.000	0.000	0.000	0.981	16.239	27.140	0.996	16.239	14.923
	SVM	0.999	1.659	6.036	0.991	8.039	19.367	0.998	9.699	11.782
Nov	ANN	1.000	0.088	1.105	0.992	9.859	25.060	0.997	9.947	13.810
	SVM	0.999	1.519	5.907	0.998	4.376	16.489	0.999	5.895	10.322
Dec	ANN	0.999	5.546	11.266	0.987	13.126	29.161	0.996	18.672	18.591
	SVM	1.000	1.486	5.310	0.996	5.581	17.910	0.999	7.067	10.800
Jan	ANN	1.000	0.122	1.642	0.958	27.209	42.839	0.991	27.332	23.595
	SVM	1.000	0.265	2.497	0.992	5.453	20.200	0.998	5.717	11.301
Feb	ANN	0.994	12.746	18.127	0.911	87.638	76.617	0.968	99.861	44.338
	SVM	1.000	0.002	0.194	0.938	58.815	56.751	0.984	58.817	30.848
Mar	ANN	1.000	0.775	4.137	0.900	82.512	65.843	0.969	83.251	35.957
	SVM	0.993	8.544	15.800	0.920	86.432	65.742	0.970	94.958	38.116
Apr	ANN	1.000	0.073	1.418	0.910	54.068	53.239	0.969	54.141	28.963
	SVM	0.995	2.640	9.171	0.957	26.030	37.591	0.981	28.670	21.835
May	ANN	1.000	0.000	0.000	0.845	23.190	38.442	0.967	23.190	20.896
	SVM	0.999	0.702	4.026	0.929	10.622	25.992	0.984	11.324	14.527
Jun	ANN	0.993	9.733	13.941	0.935	31.964	40.607	0.971	37.802	24.982
	SVM	1.000	0.001	0.132	0.975	12.623	27.322	0.991	12.624	14.851
Jul	ANN	0.994	17.670	17.879	0.974	42.065	49.212	0.984	59.668	30.672
	SVM	0.993	19.374	18.773	0.985	20.648	33.186	0.990	39.332	23.952
Aug	ANN	1.000	0.000	0.066	0.948	55.084	48.487	0.987	55.085	26.356
	SVM	0.985	38.333	25.935	0.976	49.746	48.254	0.981	88.079	34.086
Sep	ANN	1.000	0.025	0.569	0.980	26.107	37.144	0.991	26.130	20.196
	SVM	1.000	0.112	1.294	0.993	12.638	25.675	0.996	12.749	13.998
Type 1	ANN	0.985	1066.577	39.605	0.955	610.823	52.156	0.977	1677.400	43.720
	SVM	0.997	129.846	15.667	0.981	224.700	33.107	0.993	354.546	22.332
Type 2	ANN	0.983	493.066	33.022	0.974	324.422	37.400	0.983	817.487	34.384
	SVM	0.992	275.120	22.959	0.988	156.918	25.691	0.993	432.038	23.805

current period as input variable has only a negligible effect on the results of the SVM model. In other words, the non-forecasting SVM model has higher accuracy than its forecasting model.

Reservoir releases calculated with the forecasting and non-forecasting approach in type 1 and type 2 data using ANN, SVM, and NLP in the months of October through September are shown in Figs. 3, 4, 5, 6, 7, 8, 9, and 10, in which the reservoir releases calculated with NLP are named "Release Lingo." It is obvious that in all months except October, the maximum release is achieved in some years. The forecasting approach with type 2 data exhibited the best performance in all months. The ANN model with type 1 and type 2 data displayed the largest deviations from the NLP solutions. Overall, type 2 data

Table 6 Average statistics of *R*, *ME*, and *RMSE* for the forecasting and non-forecasting approaches

Implementation	*R* (%)	*ME* (10^6 m^3)	*RMSE* (10^6 m^3)
Non-forecasting with SVM	0.986	55.33	20.70
Non-forecasting with ANN	0.975	143.26	27.32
Forecasting with SVM	0.980	67.63	25.03
Forecasting with ANN	0.960	179.65	40.11

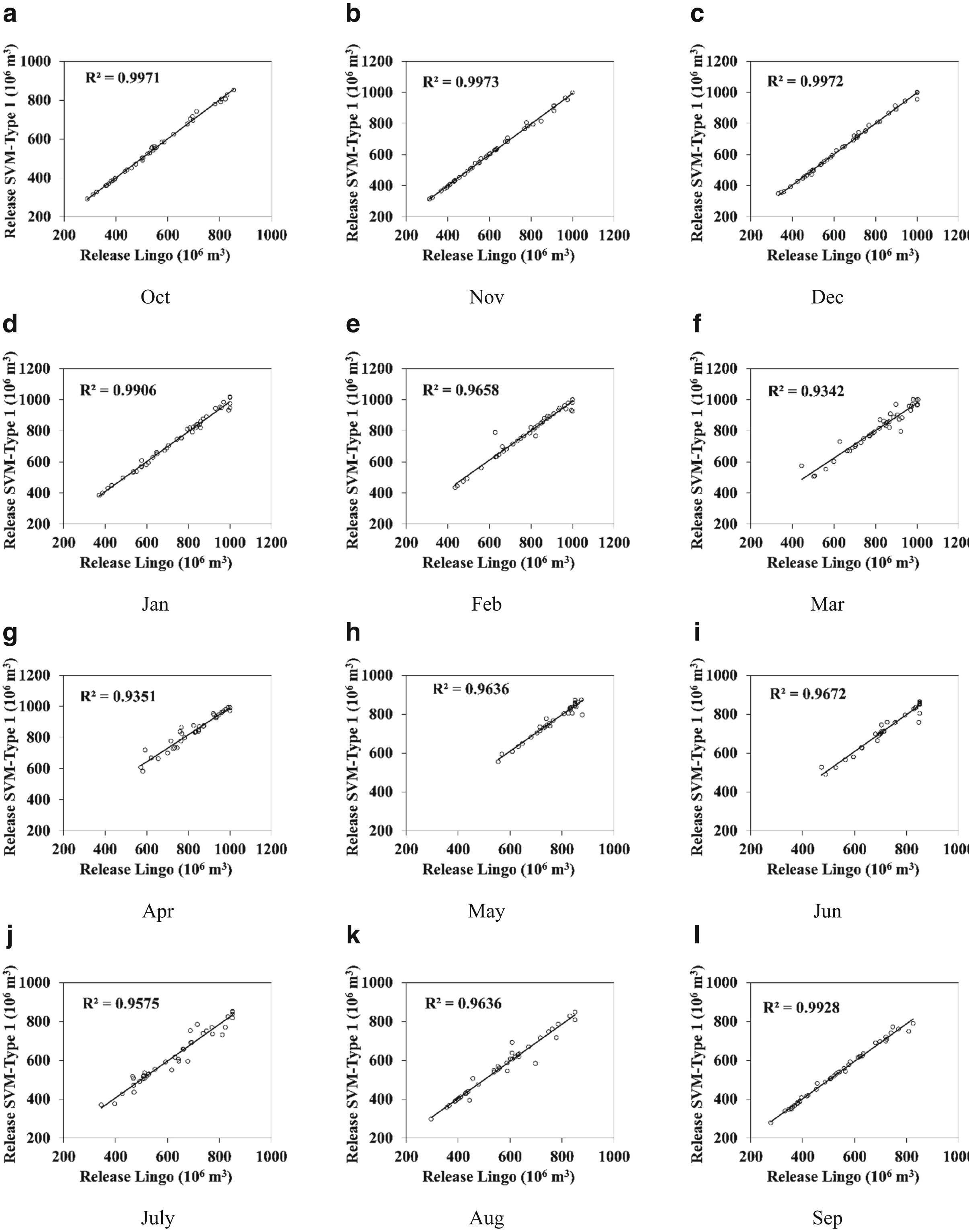

Fig. 3 Reservoir releases calculated with the non-forecasting approach in (**a**) October through (**l**) September for SVM type 1 data and NLP models

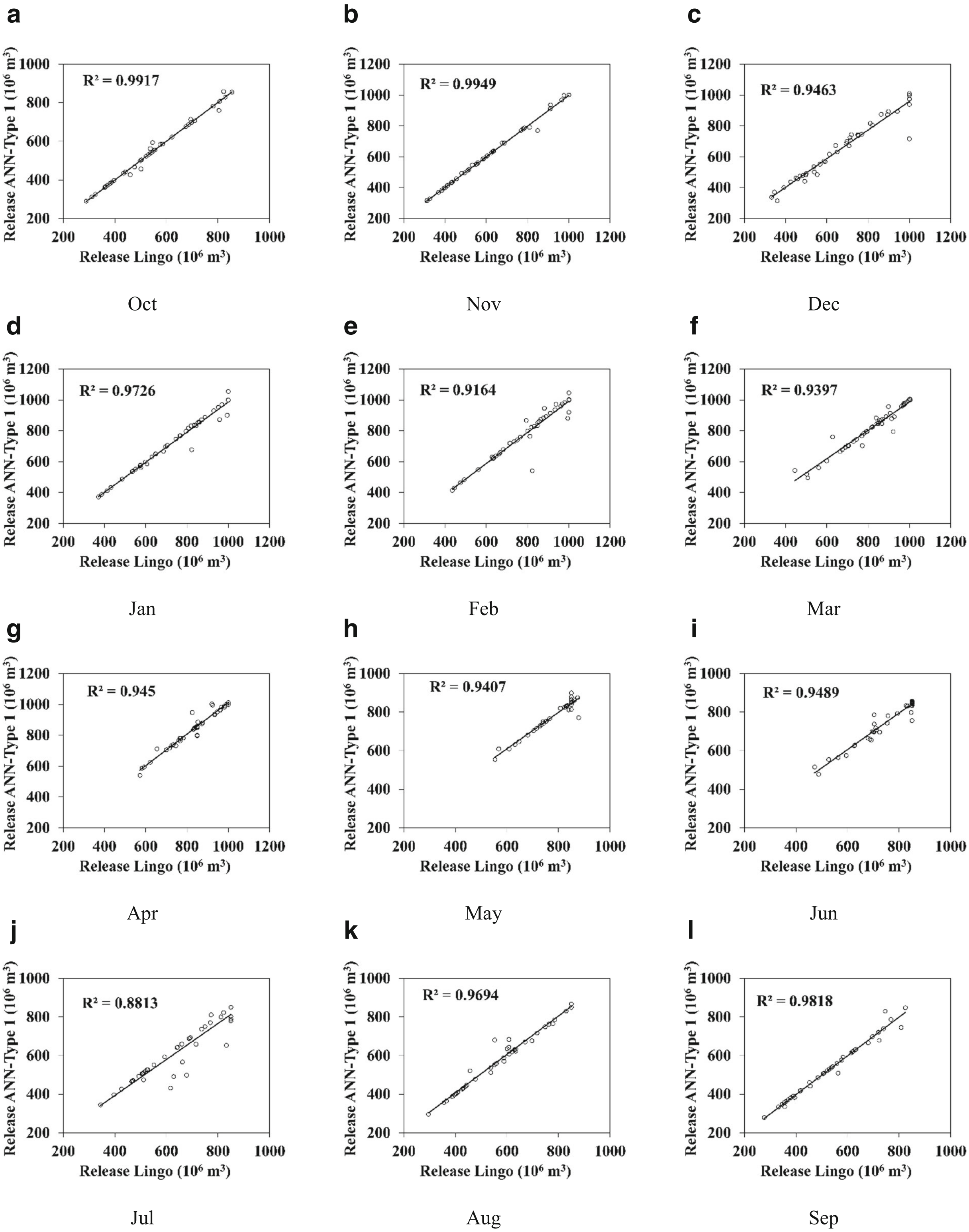

Fig. 4 Reservoir releases calculated with the non-forecasting approach in (**a**) October through (**l**) September for ANN type 1 data and NLP models

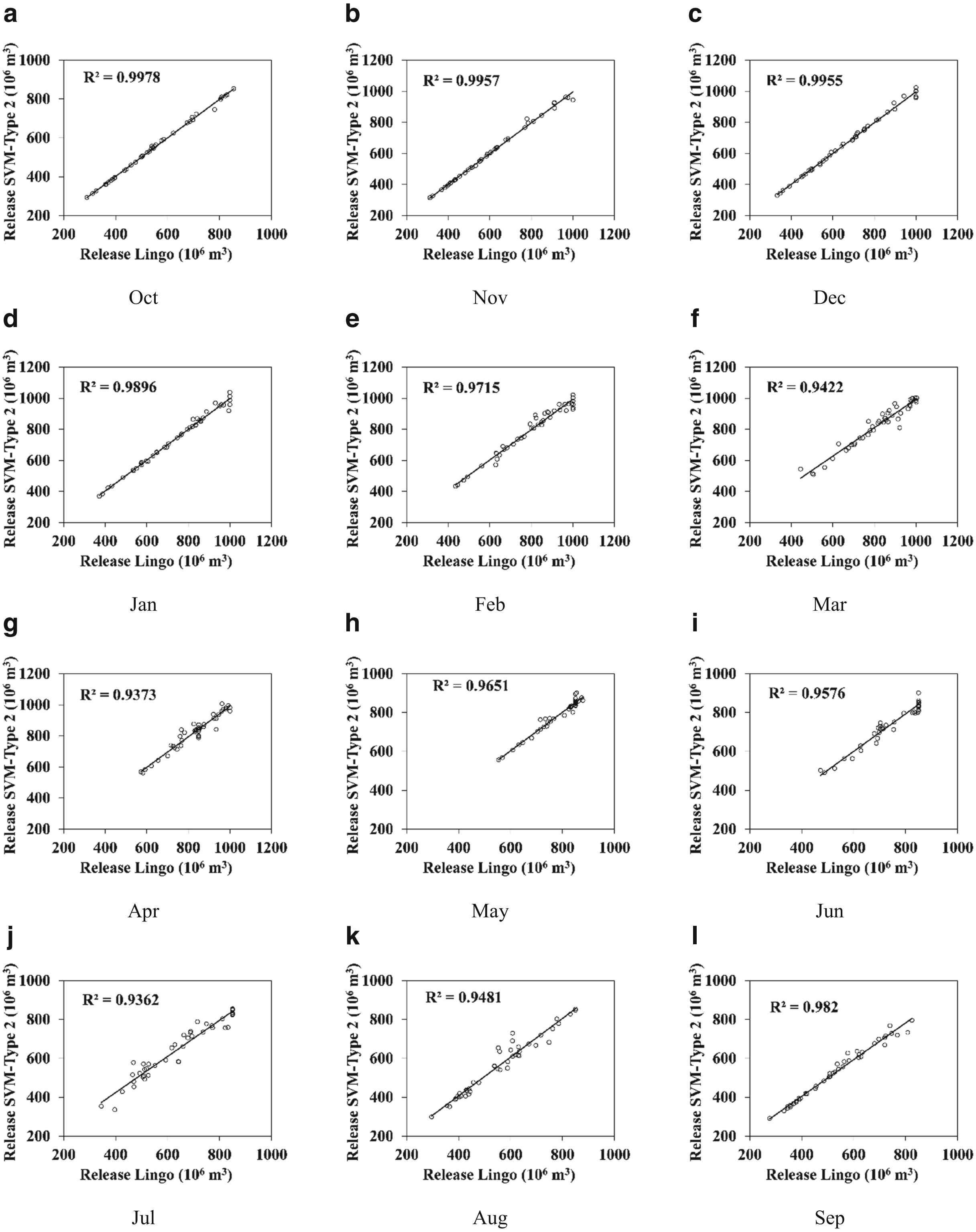

Fig. 5 Reservoir releases calculated with the non-forecasting approach in (**a**) October through (**l**) September for SVM type 2 data and NLP models

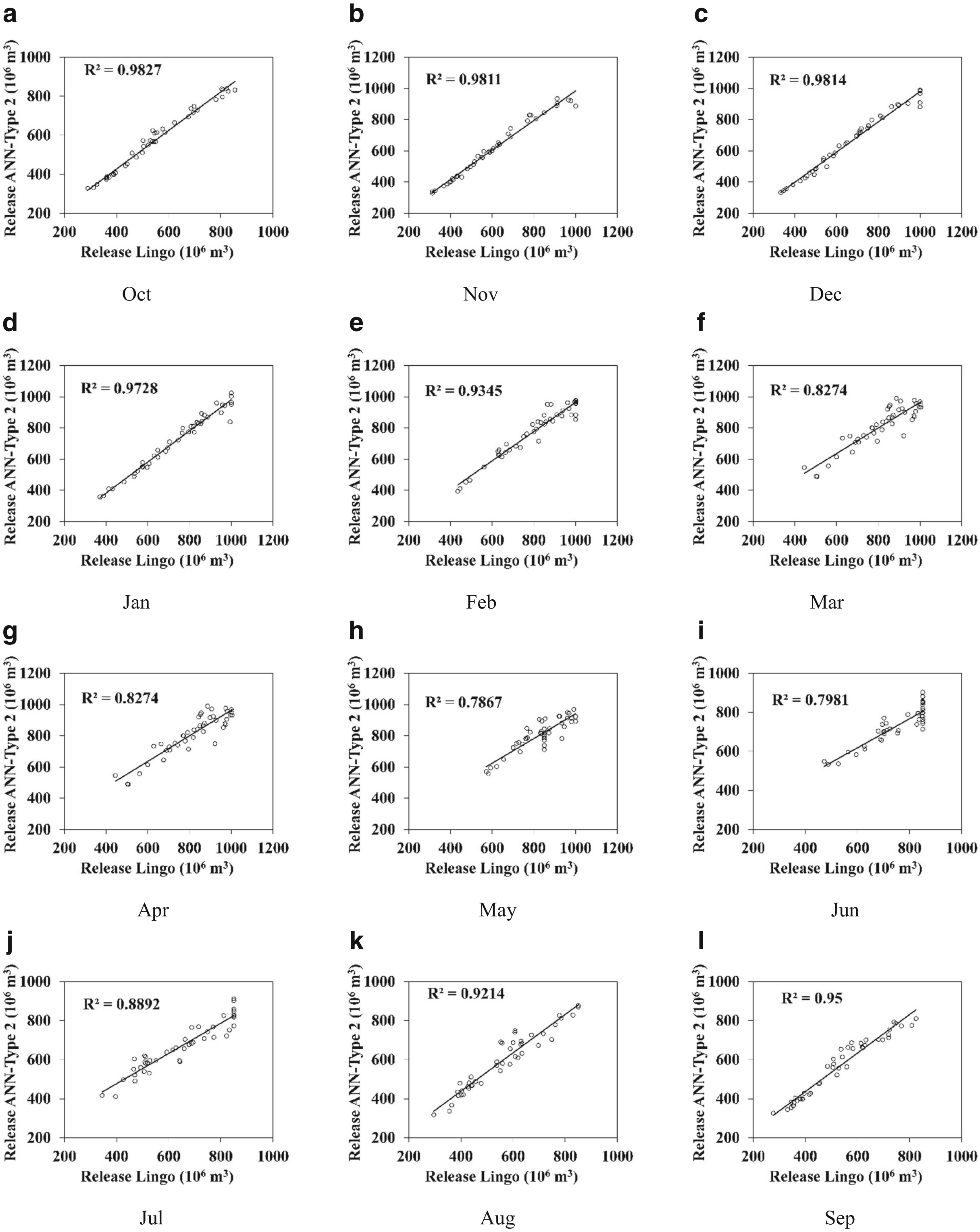

Fig. 6 Reservoir releases calculated with the non-forecasting approach in (**a**) October through (**l**) September for ANN type 2 data and NLP models

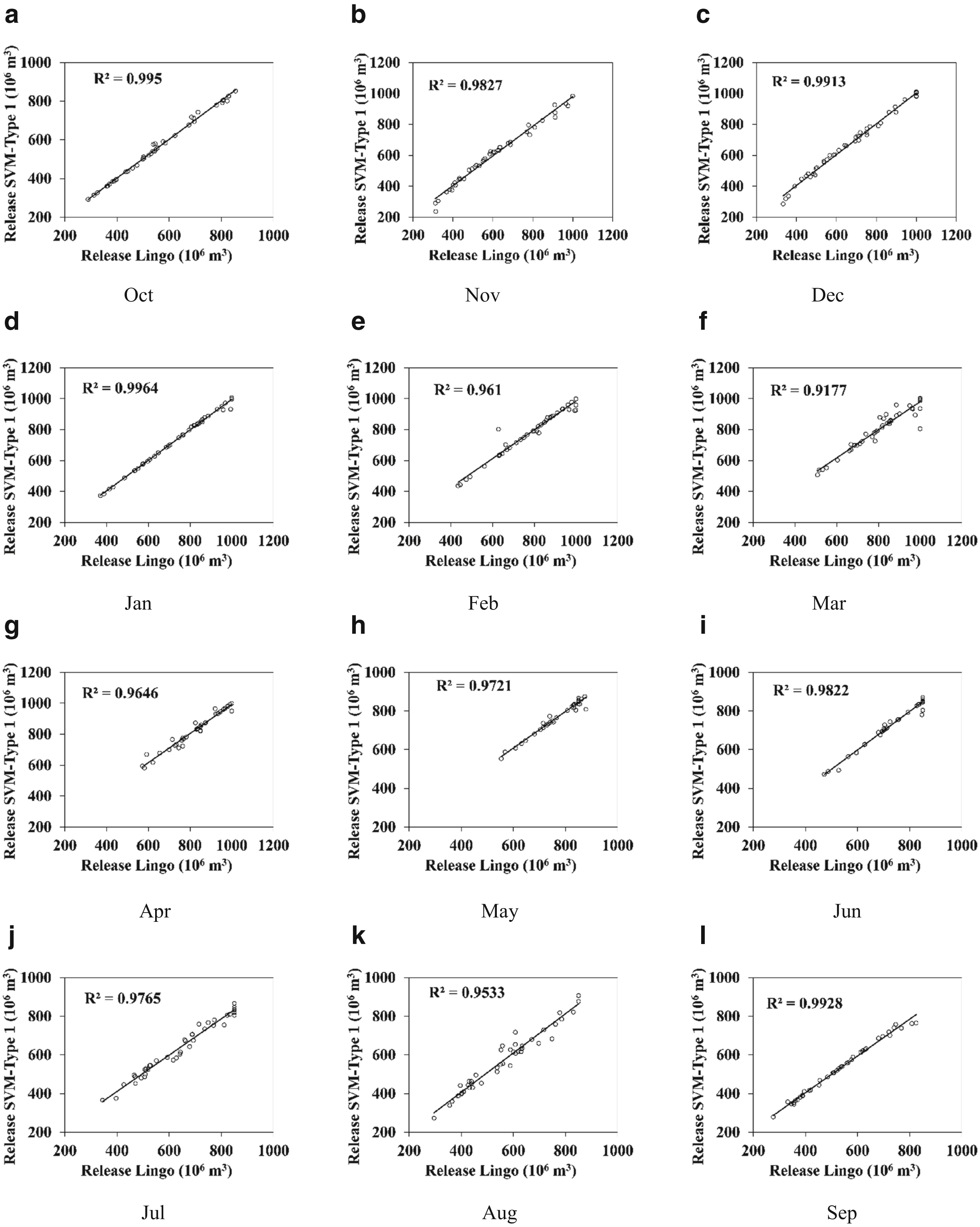

Fig. 7 Reservoir releases calculated with the forecasting approach in (**a**) October through (**l**) September for SVM type 1 data and NLP models

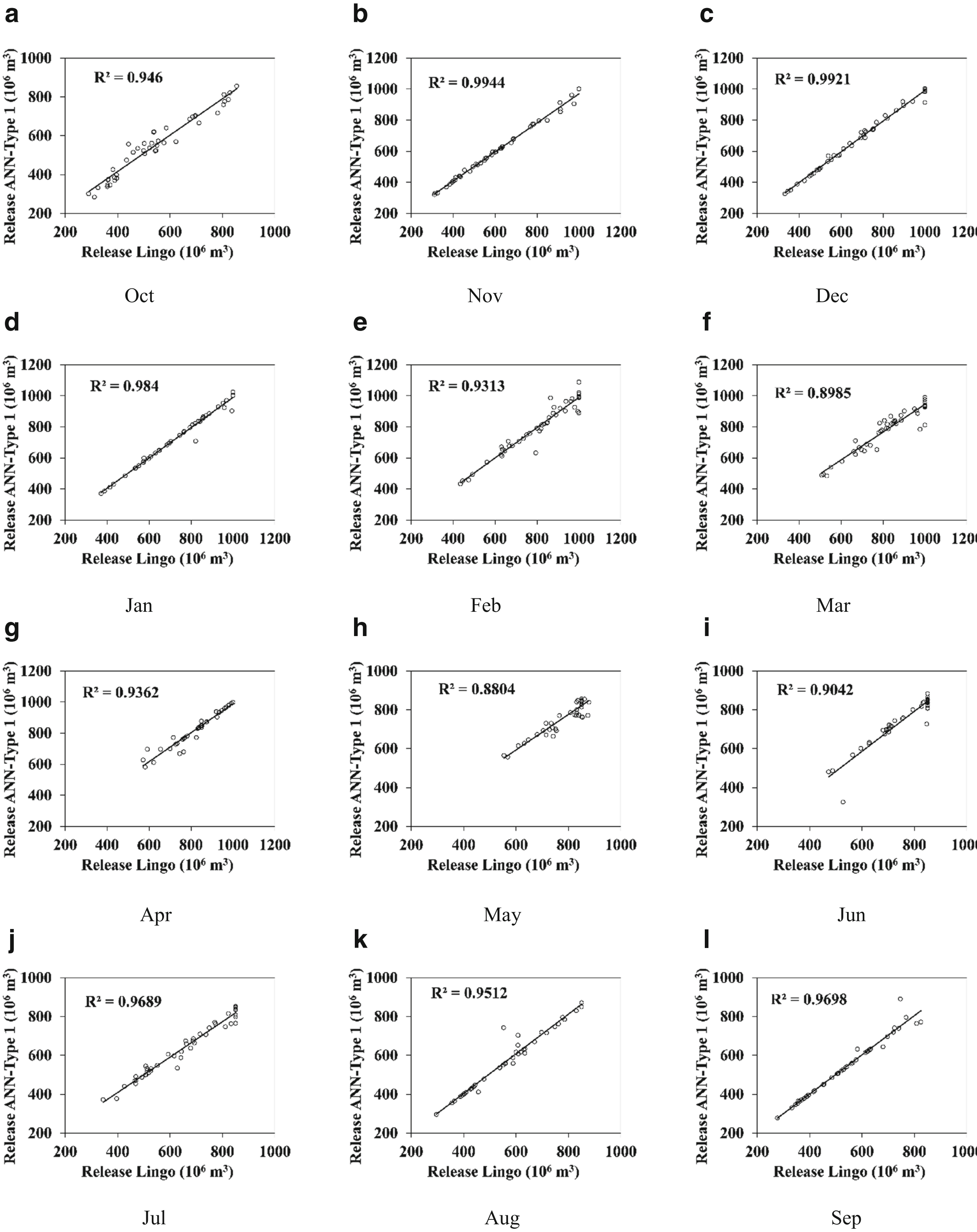

Fig. 8 Reservoir releases calculated with the forecasting approach in (**a**) October through (**l**) September for ANN type 1 data and NLP models

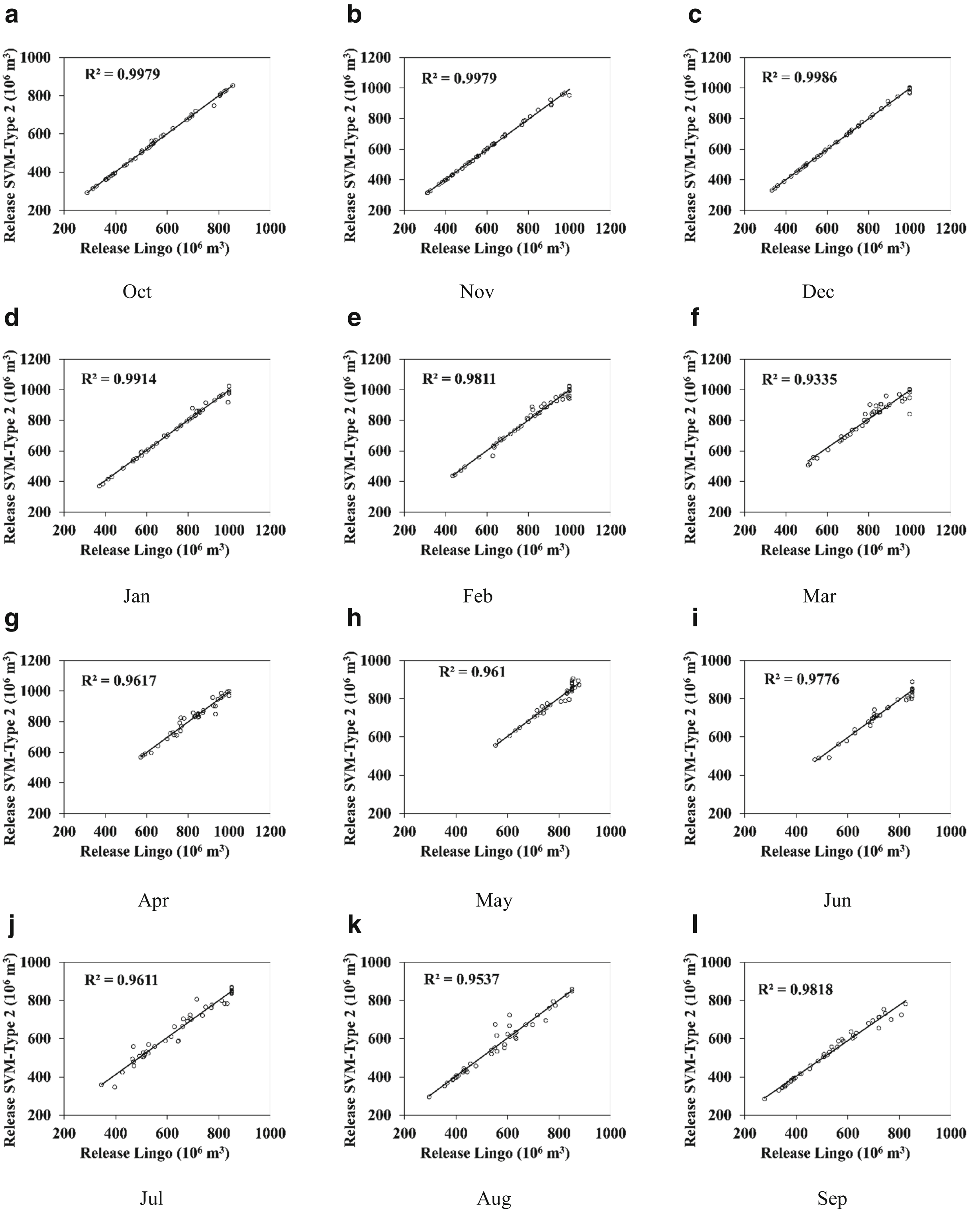

Fig. 9 Reservoir releases calculated with the forecasting approach in (**a**) October through (**l**) September for SVM type 2 data and NLP models

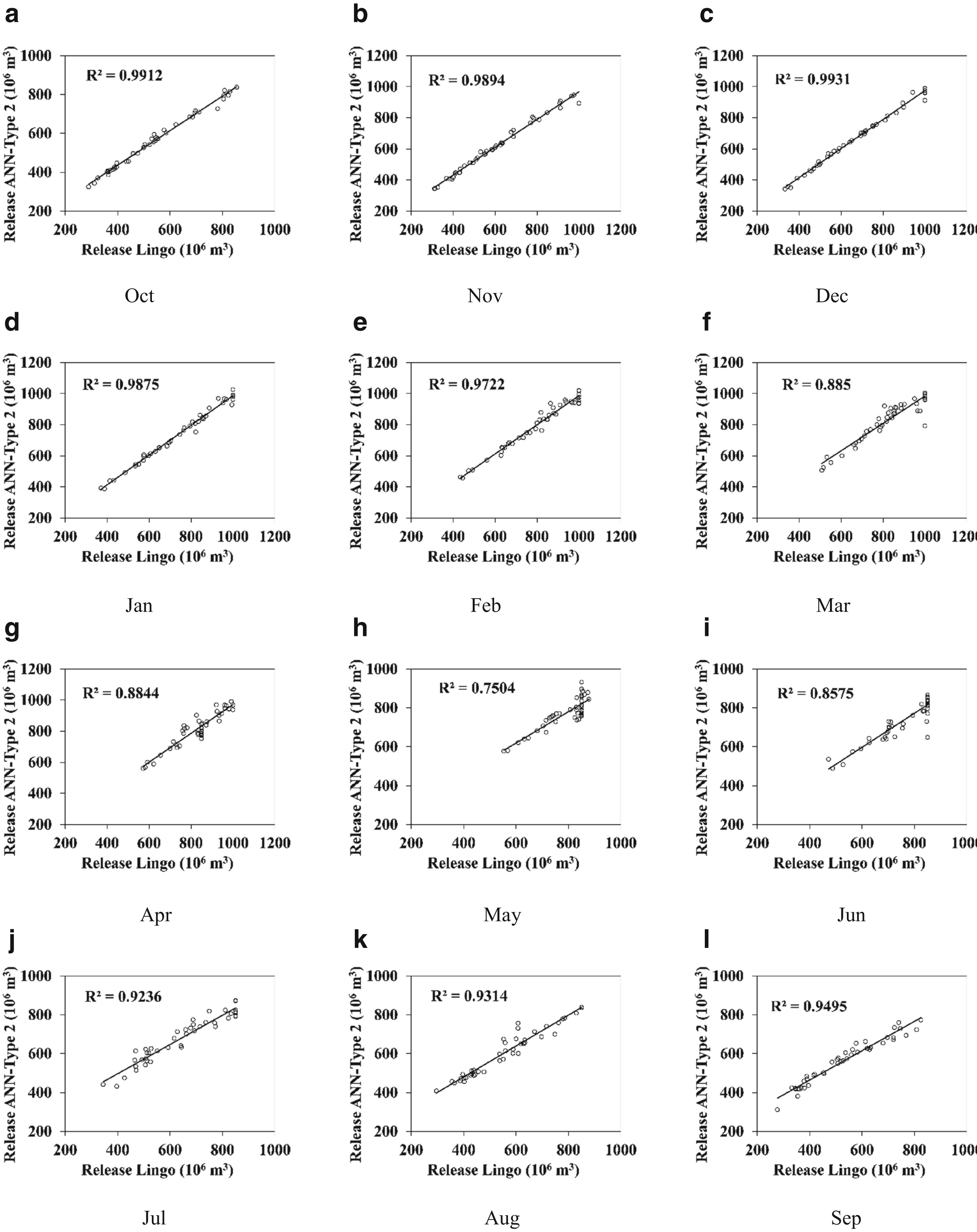

Fig. 10 Reservoir releases calculated with the forecasting approach in (**a**) October through (**l**) September for ANN type 2 data and NLP models

performed better than type 1 data of the latter finding is accentuated in January, February, and March with the ANN model. It is seen that the calculated releases deviate most from the NLP-calculated releases in April and July. The calculated releases with ANN and type 1 data deviate most from the NLP values in all months, except in July, when ANN with type 2 data exhibited the release with the largest deviation from NLP. Except for July, the reservoir release did not achieve maximum in the months April through September. This is explained by the drier seasons comprised within April through September. The testing phase results were poorer than those of the training phase, with the deviation between model-calculated releases and NLP releases being more pronounced in July and August. In general, performance of the type 2 data was better than that of the type 1 data with the ANN and SVM models.

Moreover, Figs. 3, 4, 5, 6, 7, 8, 9, and 10 demonstrate the prediction error in this case is smaller than that observed with the non-forecasting approach. The best and worst predictions compared with NLP occurred in January and March, respectively. The SVM model performed better than ANN in March. There is an obvious deviation between the ANN with type 1 data-calculated releases from those calculated with NLP when the non-forecasting approach is implemented, something that does not occur with the releases calculated with ANN and type 1 data when implementing the forecasting approach.

The forecasting approach in April through September reveals that the calculated releases exhibit smaller errors than those observed with the non-forecasting approach. The best and worst performances are observed in June and July, respectively, when compared with the NLP-calculated releases. Despite the large deviation in July, the SVM forecasting model performed better than ANN. Also, the ANN forecasting model with type 1 and type 2 data exhibited larger deviations from the NLP results than the SVM model.

Concluding remarks

The SVM and ANN models were applied to determine optimal releases from the Karoon 3 reservoir using as inputs the results obtained with NLP. The training and testing data were selected for both models with percentages equal to 70% and 30%, respectively, randomly. Forecasting and non-forecasting scenarios were considered to assess the accuracy of SVM and ANN without requiring the information necessary to apply NLP. Input variables to the forecasting approach were the reservoir storage and inflow volume in the current period and the three previous periods. Input variables to the non-forecasting approach were the reservoir storage in the current period and the three previous time periods and reservoir inflow in the three periods prior to the current period. The reservoir release was considered as the output variable. The impact of data integration on the models' performances was assessed with multiple runs involving type 1 data (long-term time series data), type 2 data (monthly data), two modeling approaches (forecasting and non-forecasting approaches), and implemented with the ANN and the SVM models. Three diagnostic statistics (*R*, *ME*, and *RMSE*) were calculated to evaluate the models' results. The results showed that (1) the SVM and ANN models calculate optimal release of hydropower reservoirs with accuracy, (2) the SVM model has better performance than the ANN model, (3) the use of monthly data (type 2 data) improves the performance of the SVM and ANN models, and (4) the non-forecasting approach performs very well compared with the forecasting approach, despite the lack of use in the former approach of reservoir inflow in the current period as an input variable to calculate reservoir release. These results reveal the superiority of SVM and ANN over NLP for the given application. The data mining techniques require NLP output for training procedure; yet, they reach suitable results without the information that NLP requires. It is worthy of mention that the use or lack of use of reservoir inflow in the current period as input variable had less effect on the results of the SVM model than it did on those of the ANN model. In other words, the non-forecasting approach with SVM had better accuracy than the non-forecasting and forecasting approaches applied with ANN.

Acknowledgments The authors thank Iran's National Science Foundation (INSF) for its financial support of this research.

References

Aboutalebi, M., & Bozorg-Haddad, O. (2015). Support vector machine with non-dominated sorting genetic algorithm for the monthly inflow prediction in hydropower reservoir. *International Journal of Civil and Structural Engineering, 2*(1), 239–242.

Aboutalebi, M., Bozorg-Haddad, O., & Loáiciga, H. A. (2015). Optimal monthly reservoir operation rules for hydropower generation derived with SVR-NSGAII. *Journal of Water Resources Planning and Management, 141*(11). https://doi.org/10.1061/(ASCE)WR.1943-5452.0000553.

Aboutalebi, M., Bozorg-Haddad, O., & Loáiciga, H. A. (2016a). Application of the SVR-NSGAII to hydrograph routing in open channels. *Journal of Irrigation and Drainage Engineering, 142*(3). https://doi.org/10.1061/(ASCE)IR.1943-4774.0000969.

Aboutalebi, M., Bozorg-Haddad, O., and Loáiciga, H.A., (2016b). Multi-objective design of water-quality monitoring networks in river-reservoir systems. *Journal of Environmental Engineering*, 04016070. https://doi.org/10.1061/(ASCE)EE.1943-7870.0001155.

Aboutalebi, M., Bozorg-Haddad, O., & Loáiciga, H. A. (2016c). Simulation of methyl tertiary butyl ether (MTBE) concentrations in river-reservoir systems using support vector regression (SVR). *Journal of Irrigation and Drainage Engineering, 142*(6). https://doi.org/10.1061/(ASCE)IR.1943-4774.0001007.

Ahmadi, A., Han, D., Kakaei-Lafdani, E., & Moridi, A. (2015a). Input selection for long-lead precipitation prediction using large-scale climate variables: a case study. *Journal of Hydroinformatics, 17*(1), 114–129. https://doi.org/10.2166/hydro.2014.138.

Ahmadi, M., Bozorg-Haddad, O., & Loáiciga, H. A. (2015b). Adaptive reservoir operation rules under climatic change. *Water Resources Management, 29*(4), 1247–1266.

Akbari-Alashti, H., Bozorg-Haddad, O., Fallah-Mehdipour, E., & Mariño, M. A. (2014). Multi-reservoir real-time operation rules: a new genetic programming approach. *Proceedings of the Institution of Civil Engineers: Water Management, 167*(10), 561–576.

Asefa, T., Kemblowski, M., Urroz, G., McKee, M., & Khalil, A. (2005). Support vector machines (SVMs) for monitoring networks design. *Groundwater, 43*(4), 413–422.

Asefa, T., Kemblowski, M., McKee, M., & Khalil, A. (2006). Multi-time scale stream flow predictions: the support vector machines approach. *Journal of Hydrology, 318*(1–4), 7–16.

Babovic, V. (2004). Data mining in hydrology. *Hydrological Processes, 19*(7), 1511–1515.

Behzad, M., Asghari, K., Eazi, M., & Palhang, M. (2009). Generalization performance of support vector machines and neural networks in runoff modeling. *Expert Systems with Applications, 36*(4), 7624–7629.

Beygi, S., Bozorg-Haddad, O., Fallah-Mehdipour, E., & Mariño, M. A. (2014). Bargaining models for optimal design of water distribution networks. *Journal of Water Resources Planning and Management, 140*(1), 92–99.

Bolouri-Yazdeli, Y., Bozorg-Haddad, O., Fallah-Mehdipour, E., & Mariño, M. A. (2014). Evaluation of real-time operation rules in reservoir systems operation. *Water Resources Management, 28*(3), 715–729.

Bower, B. T., Hufschmidt, M. M., & Reedy, W. W. (1962). *Operating procedures: their role in the design of water-resource systems by simulation analyses. Design of water resources systems* (pp. 443–458). Cambridge: Harvard University Press.

Box, G. E. P., & Cox, D. R. (1964). An analysis of transformation. *Journal of the Royal Statistical Society, 26*(2), 211–252.

Bozorg-Haddad, O., Afshar, A., & Mariño, M. A. (2008a). Design-operation of multi-hydropower reservoirs: HBMO approach. *Water Resources Management, 22*(12), 1709–1722.

Bozorg-Haddad, O., Afshar, A., & Mariño, M. A. (2008b). Honey-bee mating optimization (HBMO) algorithm in deriving optimal operation rules for reservoirs. *Journal of Hydroinformatics, 10*(3), 257–264.

Bozorg-Haddad, O., Rezapour Tabari, M. M., Fallah-Mehdipour, E., & Mariño, M. A. (2013). Groundwater model calibration by meta-heuristic algorithms. *Water Resources Management, 27*(7), 2515–2529.

Bozorg-Haddad, O., Ashofteh, P.-S., and Mariño, M.A. (2015a). Levee layouts and design optimization in protection of flood areas. *Journal of Irrigation and Drainage Engineering*, 04015004. https://doi.org/10.1061/(ASCE)IR.1943-4774.0000864.

Bozorg-Haddad, O., Ashofteh, P.-S., Ali-Hamzeh, M., & Mariño, M. A. (2015b). Investigation of reservoir qualitative behavior resulting from biological pollutant sudden entry. *Journal of Irrigation and Drainage Engineering, 141*(8), 04015003. https://doi.org/10.1061/(ASCE)IR.1943-4774.0000865.

Cai, X., Mckinney, D. C., & Lasdon, L. S. (2001). Solving nonlinear water management models using a combined genetic algorithm and linear programming approach. *Advances in Water Resources, 24*(6), 667–676.

Chen, L. (2003). Real coded genetic algorithm optimization of long term reservoir operation. *Journal of American Water Resources Association, 39*(5), 1157–1165.

Cristianini, N., & Shawe-Taylor, J. (2000). *An introduction to support vector machines*. New York: Cambridge University Press.

Dibike, Y. B., Velickov, S., Solomatine, D. P., & Abbott, M. B. (2001). Model induction with support vector machines: introduction and application. *Journal of Computing in Civil Engineering, 15*(3), 208–216.

Fallah-Mehdipour, E., Bozorg-Haddad, O., Orouji, H., & Mariño, M. A. (2013a). Application of genetic programming in stage hydrograph routing of open channels. *Water Resources Management, 27*(9), 3261–3272.

Fallah-Mehdipour, E., Bozorg-Haddad, O., & Mariño, M. A. (2013b). Extraction of optimal operation rules in aquifer-dam system: a genetic programming approach. *Journal of Irrigation and Drainage Engineering, 139*(10), 872–879.

Fallah-Mehdipour, E., Bozorg-Haddad, O., & Mariño, M. A. (2014). Genetic programming in groundwater modeling. *Journal of Hydrologic Engineering, 19*(12), 04014031. https://doi.org/10.1061/(ASCE)HE.1943-5584.0000987.

Farhangi, M., Bozorg-Haddad, O., & Mariño, M. A. (2012). Evaluation of simulation and optimization models for WRP with performance indices. *Proceedings of the Institution of Civil Engineers: Water Management, 165*(5), 265–276.

Garousi-Nejad, I., & Bozorg-Haddad, O. (2015). The implementation of developed firefly algorithm in multireservoir optimization in continous domain. *International Journal of Civil and Structural Engineering, 2*(1), 104–108.

Garousi-Nejad, I., Bozorg-Haddad, O., Loáiciga, H.A., and Mariño, M.A. (2016a). Application of the firefly algorithm to optimal operation of reservoirs with the purpose of irrigation supply and hydropower production. *Journal of*

Irrigation and Drainage Engineering, 04016041. https://doi.org/10.1061/(ASCE)IR.1943-4774.0001064.

Garousi-Nejad, I., Bozorg-Haddad, O., & Loáiciga, H. A. (2016b). Modified firefly algorithm for solving multireservoir operation in continuous and discrete domains. *Journal of Water Resources Planning and Management*, 04016029. https://doi.org/10.1061/(ASCE)WR.1943-5452.0000644.

Han, D. and Cluckie, I. (2004). Support vector machines identification for runoff modeling. Proceedings of the Sixth International Conference on Hydroinformatics, 21–24 June, Singapore.

Jahandideh-Tehrani, M., Bozorg-Haddad, O., & Mariño, M. A. (2015). Hydropower reservoir management under climate change: the Karoon reservoir system. *Water Resources Management, 29*(3), 749–770.

Khalil, A., Almasri, M. N., McKee, M., & Kaluarachchi, J. J. (2005). Applicability of statistical learning algorithms in ground water quality modeling. *Water Resources Research, 41*(5), W0510. https://doi.org/10.1029/2004WR003608.

Li, X.-L., Lü, H., Horton, R., An, T., & Yu, Z. (2014). Real-time flood forecast using the coupling support vector machine and data assimilation method. *Journal of Hydroinformatics, 16*(5), 973–988. https://doi.org/10.2166/hydro.2013.075.

Lin, J.-Y., Cheng, C.-T., & Chau, K.-W. (2006). Using support vector machines for long-term discharge prediction. *Hydrological Sciences Journal, 51*(4), 599–612.

Loáiciga, H. A. (2015). Managing municipal water supply and use in water-starved regions: looking ahead. *Journal of Water Resources Planning and Management, 141*(1), 01814003/1–01814003/4.

Loucks, D. P., Stedinger, J. R., & Haith, D. A. (1981). *Water resource systems planning and analysis*. Englewood Cliffs: Prentice-Hall.

Mousavi, S. J., Ponnambalam, k., & Karray, F. (2007). Inferring operating rules for reservoir operations using fuzzy regression and ANFIS. *Fuzzy Sets and Systems, 158*(10), 1064–1082.

Oliveira, R., & Loucks, D. P. (1997). Operating rules for multireservoir systems. *Water Resources Research, 33*(4), 839–852.

Orouji, H., Bozorg-Haddad, O., Fallah-Mehdipour, E., & Mariño, M. A. (2013). Modeling of water quality parameters using data-driven models. *Journal of Environmental Engineering, 139*(7), 947–957.

Orouji, H., Bozorg-Haddad, O., Fallah-Mehdipour, E., & Mariño, M. A. (2014a). Flood routing in branched river by genetic programming. *Proceedings of the Institution of Civil Engineers: Water Management, 167*(2), 115–123.

Orouji, H., Bozorg-Haddad, O., Fallah-Mehdipour, E., & Mariño, M. A. (2014b). Extraction of decision alternatives in project management: Application of hybrid PSO-SFLA. *Journal of Management in Engineering, 30*(1), 50–59.

Pinthong, P., Gupta, D., Babel, A., & Weesakul, S. (2009). Improved reservoir operation using hybrid genetic algorithm and neurofuzzy computing. *Water Resources Management, 23*(4), 697–720.

Rakotomalala, R. (2005). TANAGRA: a free software for research and academic purposes. In Proceedings of EGC'2005, RNTI-E-3, 2, pp. 697–702.

Singh, K. P., Basant, N., & Gupta, S. (2011). Support vector machines in water quality management. *Analytica Chimica Acta, 703*(2), 152–162.

Tung, C., Hsu, S., Liu, C. M., & Li Jr., S. (2003). Application of the genetic algorithm for optimizing operation rules of the Liyutan reservoir in Taiwan. *Journal of American Water Resources Association, 39*(3), 649–657.

Vapnik, V. N. (1995). *The nature of statistical learning theory*. New York: Springer-Verlag.

Wang, W.-c., Xu, D.-m., Chau, K.-w., & Chen, S. (2013). Improved annual rainfall-runoff forecasting using PSO-SVM model based on EEMD. *Journal of Hydroinformatics, 15*(4), 1377–1390. https://doi.org/10.2166/hydro.2013.134.

Wei, C. (2012). Wavelet kernel support vector machines forecasting techniques: case study on water-level predictions during typhoons. *Expert Systems with Applications, 39*(5), 5189–5199.

Yang, T., Gao, X., Sorooshian, S., & Li, X. (2016). Simulating California reservoir operation using the classification and regression-tree algorithm combined with a shuffled cross-validation scheme. *Water Resources Research, 52*(3), 1626–1651.

Yang, T., Asanjian, A., Welles, E., Gao, X., Sorooshian, S., & Liu, X. (2017). Developing reservoir monthly inflow forecasts using artificial intelligence and climate phenomenon information. *Water Resources Research, 53*(4), 2786–2812.

Yeh, W. W. G. (1985). Reservoir management and operations models: a state of the art review. *Water Resources Research, 21*(12), 1797–1818.

Yoon, H., Jun, S., Hyun, H., Bae, G., & Lee, K. (2011). A comparative study of artificial neural networks and support vector machines for predicting groundwater levels in a coastal aquifer. *Journal of Hydrology, 39*(6), 128–138.

Yu, X., Liong, S., & Babovic, V. (2004). EC-SVM approach for real-time hydrologic forecasting. *Journal of Hydroinformatics, 6*(3), 209–223.

Yu, P.-S., Chen, S.-T., & Chang, I.-F. (2006). Support vector regression for real-time flood stage forecasting. *Journal of Hydrology, 328*(3–4), 704–716.